Eur. Phys. J. B **12**, 519–523 (1999)

THE EUROPEAN PHYSICAL JOURNAL B

EDP Sciences
© Società Italiana di Fisica
Springer-Verlag 1999

Influence of vacancies on the electronic structure of $Co_{2-x}ZrSn$ Heusler alloys

A. Ślebarski[1,a], A. Jezierski[2], M. Neumann[3], and S. Plogmann[3]

[1] Institute of Physics, University of Silesia, 40-007 Katowice, Poland
[2] Institute of Molecular Physics, Polish Academy of Sciences, 60-179 Poznań, Poland
[3] Institute of Physics, University of Osnabrück, 49069 Osnabrück, Germany

Received 9 March 1999 and Received in final form 6 May 1999

Abstract. The electronic structure of the $Co_{2-x}ZrSn$ Heusler alloys has been studied by X-ray photoelectron spectroscopy (XPS). XPS valence band spectra can be compared with *ab initio* electronic structure calculations using the linearized muffin-tin orbital (LMTO) method. The calculated magnetic moments per Co atom agree well with the moments obtained from experiment. The LMTO calculations also show the energy shifts of the Co, Zr and Sn valence electron states towards the Fermi level when the concentration of vacancies increases in these alloys.

PACS. 71.20.-b Electron density of states and band structure of crystalline solids – 71.20.Be Transition metals and alloys – 71.15.La Atomic sphere approximation methods

1 Introduction

Most of the Heusler alloys of the Cu_2MnAl-type crystallize in the $L2_1$ type cubic structure. These compounds often show ferromagnetic properties [1]. The problem of local magnetic moments, that is, localized behaviour in some aspects of the itinerant *d*-electrons, seems to be one of the most important in the physics of these materials. Among all of the itinerant-electron ferromagnets, the half-metallic ferromagnets, which includes some of the Heusler alloys, have an energy gap for one of the spin projections at the Fermi level. Mn compounds show rather localized magnetism, due to the $3d$ shell configuration of Mn [2], whereas Co compounds show more itinerant behaviour [3]. Therefore, the influence of the local environment on the magnetic properties is important in the classification of these materials. Among these alloys, Co_2MSn with M = Ti, Zr or Hf are ferromagnets [3], whereas analogous Ni compounds are Pauli paramagnets. By replacing Co by Ni it is possible to lower the Curie temperature and to pass progressively to the paramagnetic regime [4]. Another possibility is to lower the Co concentration and thus create vacancies [5]. One of the two Co sites in the $L2_1$ unit cell remains fully occupied, whereas the other Co site is replaced by vacancies, ending with CoMSn, which usually has the MgAgAs cubic structure (in the case of the series of $Co_{2-x}ZrSn$ alloys the final composition CoZrSn has a hexagonal structure of the Fe_2P-type). The reduction of the Co concentration (*e.g.* in Co_2TiSn) through vacancy creation demonstrates the classical features of itinerant magnetic magnetism [6].

The influence of the local environment on the magnetic properties in Heusler alloys has motivated us to study the electronic structure of the $Co_{2-x}ZrSn$ series. In this paper we describe experimental and theoretical studies of the electronic structures. The valence bands observed are compared with calculations. The band structure and the magnetic moments of Co are calculated by an *ab initio* spin-polarized TB LMTO method and are in good agreement with the experimentally observed values.

2 Experimental

Samples of $Co_{2-x}ZrSn$ with x in steps of 0.125, were arc melted from the constituent metals in a copper crucible in a high-purity argon atmosphere, re-melted several times and then annealed at 800 °C for 1 week. The phase purity of the samples was checked by X-ray Debye-Scherer diffraction with CuK_α radiation using a SIEMENS D-5000 diffractometer. A solid solution with the $L2_1$ structure only forms in $Co_{2-x}ZrSn$ for $x < 0.5$. For $0.5 < x < 1$ the samples are a mixture of two phases. CoZrSn crystallizes in a hexagonal structure of the Fe_2P-type. The lattice constants of $Co_{2-x}ZrSn$ are presented in Table 1. The XPS spectra were obtained with monochromatized AlK_α radiation at room temperature using a PHI 5600ci ESCA spectrometer. The total energy resolution of the electron spectra was about 0.4 eV. Binding energies were referred to the Fermi level ($\epsilon_F = 0$).

[a] e-mail: slebar@us.edu.pl

Table 1. Structural properties and results of TB LMTO band structure calculations for $Co^{I}Co^{II}_{1-x}(Vac)_xZrSn$.

	Co_2ZrSn	$Co_{1.75}ZrSn$	$Co_{1.5}ZrSn$	$Co_{1.25}ZrSn$	CoZrSn
type of structure	$L2_1$ (Refs. [5,16])	$L2_1$	$L2_1$	$L2_1$+Fe_2P $C1_b$ (LMTO)	Fe_2P
space group	$Fm\bar{3}m$	$Fm\bar{3}m$	$Fm\bar{3}m$		$P\bar{6}2m$
exp. lattice parameters in Å	6.2544	6.2331	6.1943	6.000 (calc.)	$a = 7.1594$ $c = 3.5906$
DOS at ϵ_F in states/(eV cell)	3.38	3.39	2.48	0.27	0.99
DOS at ϵ_F in states/(eV atom)	0.85	0.85	0.36	0.067	0.33
magnetic moment per formula unit	1.74 (1.81*)	1.09 (1.22*)	0.56	0	Pauli paramagnet*
from LMTO in μ_B	μ(Co) = 0.94 (0.8*)	0.55, (0.58*) $\mu(Co^I) = 0.86$	0.46	0	0
	μ(Zr) = −0.14	−0.12	−0.10	0	0
	μ(Sn) = 0	0	0	0	0
Wigner-Seitz radii S_n/S	0.89	0.9	0.9	0.9	0.8
for: Co, Zr and Sn	1.13	1.14	1.14	1.14	1.05
	1.04	1.05	1.07	1.12	1.09

* The experimental value in bracket is from reference [5].

The electronic structures of the Heusler alloys were calculated using the spin-polarized self-consistent TB LMTO method [7], within the framework of the local spin density (LSD) approximation. The von Barth-Hedin form of the exchange correlation potential [8] was used. The self consistent calculations were performed in the atomic sphere approximation (ASA) and the standard combined corrections [7] for the overlapping of the spheres were applied. The self-consistent band calculations were carried out for more than 200 k-points in the irreducible wedge of the Brillouin zone. The values of the atomic spheres radii were taken in such a way that the sum of all atomic sphere volumes was equal to the volume of the unit cell ($\sum_n (S_n/S)^3 = N$, where $S = a(3/4\pi N)^{1/3}$, a denotes the lattice parameter, N is the number of atoms in the cell, and the summation was made for all atoms in the cell). In these calculations the ratio of the Wigner-Seitz radii S_n/S for Co, Zr and Sn atoms almost does not depend on x in $Co_{2-x}ZrSn$ (Tab. 1). The values of the atomic potentials at the sphere boundary were similar for all atoms, and the overlapping of the spheres was less than 9%. We observed a slight influence of S_{Co}/S on the calculated Co-magnetic moment, however, in our calculations we chose the atomic radii of atoms in such a way that the overlapping of the sphere was less. In consequence, the values of the atomic potential on the sphere boundary were similar and the total energy of the alloy x was the least. The cubic $L2_1$ structure of $Co_{2-x}ZrSn$ ($Co^ICo^{II}_{1-x}(Vac)_xZrSn$) consists of four interpenetrating fcc sublattices with the origins at (000)Zr, $(\frac{1}{2}\frac{1}{2}\frac{1}{2})$Sn, $(\frac{1}{4}\frac{1}{4}\frac{1}{4})$Co and $(\frac{3}{4}\frac{3}{4}\frac{3}{4})$Co or empty sphere (Vac). The calculations were performed for the structural model in which each fcc sublattice was replaced by a supercell sublattice. In this way we have a 16-atom unit cell for $Co^ICo^{II}_{1-x}(Vac)_xZrSn$. The disorder was considered only in one fcc sublattice. Co^I was located at $(\frac{1}{4}\frac{1}{4}\frac{1}{4})$ atomic positions, whereas the disordered $(\frac{3}{4}\frac{3}{4}\frac{3}{4})$ sublattice was occupied by Co^{II} or (Vac). For $x = 0$, 0.25 and 0.5 the band calculations were performed for the lattice parameters taken from the X-ray diffraction. The alloy $x = 0.75$ does not exist. The X-ray diffraction pattern shows a mixture of two phases, one of the $L2_1$-type and the second of the Fe_2P-type. For the hypothetical alloy $x = 0.75$ we calculated the lattice parameter (Tab. 1) that corresponds to the minimum of the total energy for a cubic $C1_b$-type structure.

3 Results and discussion

The valence band (VB) XPS spectra of $Co_{2-x}ZrSn$ alloys are presented in Figure 1. A background, calculated by a Tougaard algorithm [9] was subtracted. The bands extend from the Fermi energy $\epsilon_F = 0$ to a binding energy of about 10 eV. The spectra show a major peak located at about 2 eV for Co_2ZrSn which slightly shifts towards ϵ_F with increasing lattice vacancies. A second peak in the Co_2ZrSn spectra is located at about 9 eV and also shifts towards ϵ_F with increasing x.

In Figure 1 a comparison of the LMTO valence band calculations with XPS spectra is shown, which demonstrates a good agreement in each case. The DOS are convoluted by Lorentzians with a half-width of 0.4 eV. The partial DOS were multiplied by the corresponding cross

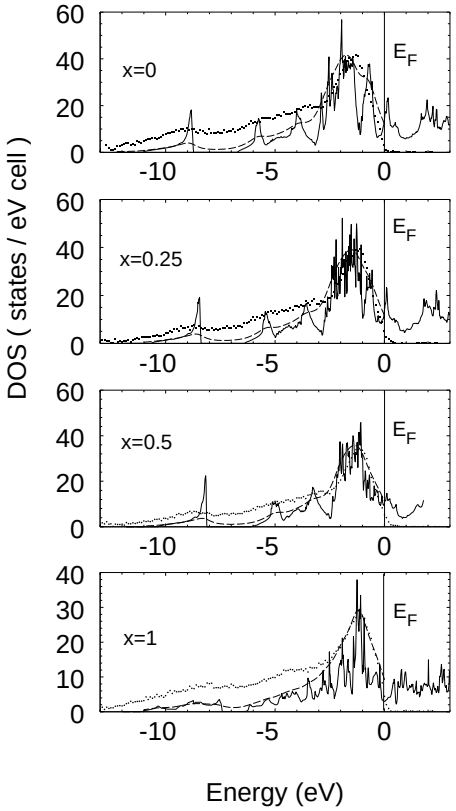

Fig. 1. Valence band XPS spectra (points), the inelastic background was subtracted. Total DOS (solid line) and convoluted DOS by Lorentzians with a half-width of 0.4 eV taking into account proper photoelectronic cross-sections for partial bands (dashed line) for $Co_{2-x}(Vac)_xZrSn$. The Fermi level is marked by a dotted line at $E = 0$ eV.

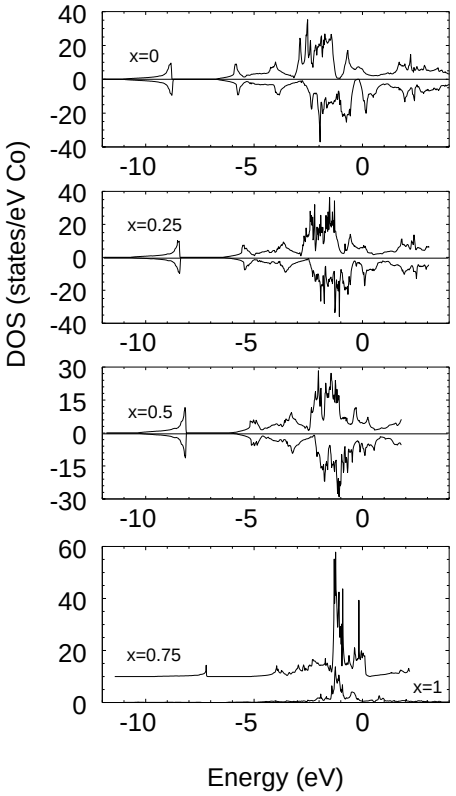

Fig. 2. Spin-projected DOS of Co for ferromagnetic $Co_{2-x}(Vac)_xZrSn$, $x = 0$, 0.25 and 0.5 (upper part). Total DOS of Co for the paramagnetic alloys $x = 0.75$, 1 (lower part).

sections, which are taken from reference [10]. The peaks located near ϵ_F in the XPS VB spectra are mainly attributed to d states of Co. The second peak at about 9 eV represents mainly Sn valence electronic states.

In Figures 2–4 we show the partial DOS of the Co, Zr and Sn states in $Co_{2-x}(Vac)_xZrSn$ alloys. The DOS maxima shift towards ϵ_F when x increases. However, Figure 1 shows that the shift of the calculated DOS maxima is about 0.5 eV while the experimentally observed shift is only about 0.1 eV, which should be considered within the experimental error. We present the following explanation. In Heusler-type alloys the electronic structure strongly depends on the local ordering. The calculated spectra which are presented in Figure 1 have not been obtained for the real crystallographic disorder, and the disagreement can be substantial when they are compared with the respective XPS valence bands.

The band calculations for Co_2ZrSn (Fig. 2) show an energy gap for one of the spin projections about 0.2 eV below the Fermi level, however the DOS has comparable magnitude for both up- and down-spins at ϵ_F. Therefore, Co_2ZrSn is not classified as a half-metallic ferromagnet, which always has an energy gap for one of the spin projections at the Fermi level. For $x = 0.25$ the pseudogap for one spin direction is located in the band almost at

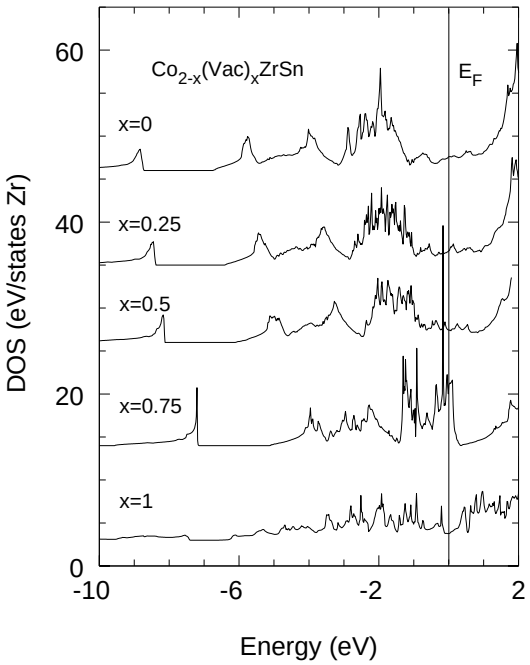

Fig. 3. Total DOS of Zr for $Co_{2-x}(Vac)_xZrSn$.

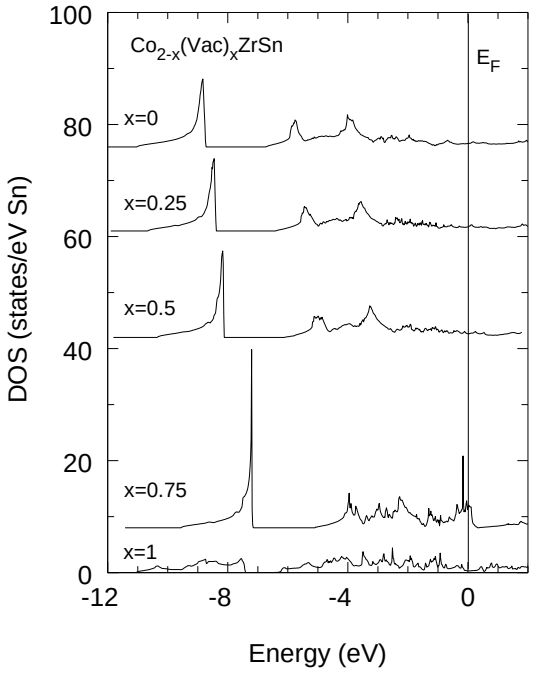

Fig. 4. Total DOS of Sn for $Co_{2-x}(Vac)_xZrSn$.

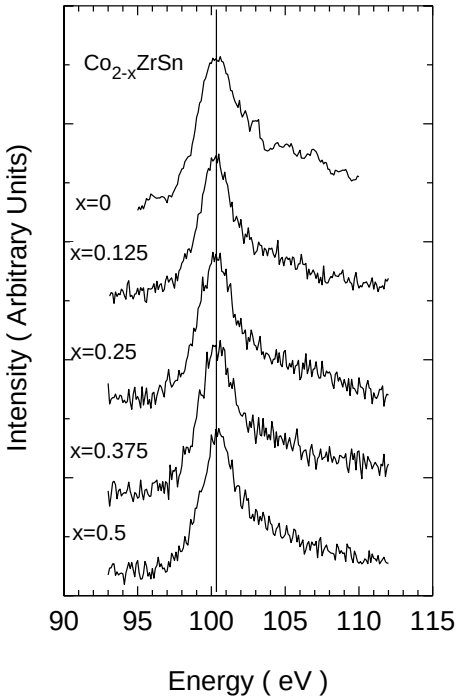

Fig. 5. Co 3*s* XPS spectra for $Co_{2-x}(Vac)_xZrSn$ alloys, $x < 0.5$.

the same energy and the up- and down-spin densities are almost equal for Co. A similar behaviour near the Fermi level is also observed for the more deficient sample $x = 0.5$. Furthermore, as the magnetic splitting decreases with x (Tab. 1), a half-metallic behaviour does not occur even for Co_2ZrSn. The LMTO calculations were carried out for $Co^{I}_{1}Co^{II}_{1-x}(Vac)_xZrSn$ with a fully occupied Co^{I} sublattice and disordered occupation of the Co^{II} sites. The calculated magnetic moments per Co atom well agree with the magnetic moments obtained from the saturated magnetization (Tab. 1) and are always smaller than $1\mu_B$. The experimentally determined Rhodes-Wohlfarth ratio μ_{eff}/μ_{sat} is considerably larger than unity and decreases as a function of the Curie temperature [5] (μ_{eff}(Co) is deduced from the Curie constant, μ_{sat}(Co) is the magnetic moment in the ground state obtained from saturation magnetization). Pierre *et al.* [6] discussed the μ_{eff}/μ_{sat} ratio in $TiCo_{2-x}Sn$, which for these Heusler compounds falls nearly exactly on the Rhodes and Wohlfarth curve obtained for Fe, Co and Ni alloys in agreement with the general trend for the itinerant systems. The effective paramagnetic moment in the classical explanation can be related to the band structure and to local correlations, however, the ordered moment depends more rapidly on the intersite interactions. The creation of vacancies should, however, decrease the overlap between Co atoms, giving narrower bands and an increased tendency to form local magnetic moments. Thus, decreasing the Co content produces increases of the mean distances between Co-atoms. This should not favour the occurrence of the band magnetism, but reduces the exchange interaction, as in fact has been observed since the Curie temperature falls. For the alloys with $x > 0.5$ no gap has been observed in the *d* bands, and the ground state is paramagnetic. The calculations predict an unstable hexagonal structure for CoZrSn. This also may be the reason why the VB XPS spectra of the sputtered CoZrSn sample resemble the VB XPS spectra of the more stable structure of Co_2ZrSn [11].

Figure 5 displays the XPS spectra of the Co 3*s* level for the Co-rich $Co_{2-x}ZrSn$ alloys. From least-squares fits of these XPS spectra using a single Doniach-Šunjić line [12] for the main component and subtracting a Tougaard background, a second peak at 4.2 eV higher binding energy was detected. The intensity ratio for the deconvoluted peaks was 0.05. The half-width of both lines was 1.9 eV. Recently, spin polarized photoemission was used to study the 3*s* core level spectra of Fe and Co single crystals [13–15]. The spin integrated spectrum of Co(001) shown in reference [15] is similar to the Co 3*s* spectra in Figure 5. In reference [15] configuration interactions were predicted, which determine the relative splitting between the low and high spin states. It also seems to be possible to obtain site specific spin moment information from the 3*s* spectra. From the XPS spectra presented in Figure 5 we only can speculate about the spin splitting of the Co 3*s* level in the Co-rich alloys. Such simple peak fitting gives a very small intensity ratio for the deconvoluted peak, and we therefore only carefully suggest the splitting.

4 Conclusions

A defect solid solution is found in $Co_{2-x}ZrSn$ for $x < 0.5$. X-ray diffraction studies showed the $L2_1$-type structure for $x < 0.5$ and the Fe_2P-type structure for the CoZrSn alloy. Co_2ZrSn is ferromagnetic, the reduction of Co concentration through vacancy creation decreases the Curie

temperature and the saturated magnetic moment. CoZrSn is a Pauli paramagnet. For the alloys with $x = 0.25$ and 0.5 the electronic structure calculations gave a pseudogap located at about 0.2 eV below the Fermi level, however at ϵ_F the up- and down-spin densities are almost equal for Co. CoZrSn has a low DOS at ϵ_F and its hexagonal structure is not stable in calculations of the total energy. The LMTO calculations show an energetic shift of the Co, Zr and Sn valence electron states towards ϵ_F, when the concentration of Co decreases in the alloys.

The magnetic moments, as obtained from calculations, agree well with the results of the saturation magnetization. The 3*s* Co XPS spectra in the $Co_{2-x}ZrSn$ series are similar for all magnetic alloys and are comparable with the spin-polarized photoemission studies [15] of a Co single crystal.

This work was partly supported by the Deutscher Akademischer Austausch Dienst (DAAD) and by the Deutsche Forschungsgemeinschaft (DFG). One of us (A.J.) thanks the State Commitee for Scientific Research for financial support (Project No. P03B02715). The calculations were made in the Supercomputing and Networking Centre of Poznań.

References

1. P.J. Webster, K.R.A. Ziebeck, in *Magnetic Properties of Metals* (Springer, Berlin, 1988), Landolt-Börnstein New Ser. 1, Group III, Vol. 19c, p. 75.
2. J. Kübler, A.R. Williams, C.B. Sommers, Phys. Rev. B **28**, 1745 (1983).
3. K.R.A. Ziebeck, P.J. Webster, J. Phys. Chem. Solids **35**, 1 (1974).
4. J. Pierre, R.V. Skolozdra, Yu.K. Gorolenko, M. Kouacou, J. Magn. Magn. Mater. **134**, 95 (1995).
5. R.V. Skolozdra, Yu.V. Stadnyk, Yu.K. Gorolenko, E.E. Terletskaya, Fiz. Tverd. Tela **32**, 2650 (1990) [Sov. Phys.-Solid State **32**, 1536 (1990)].
6. J. Pierre, R.V. Skolozdra, Yu.V. Stadnyk, J. Magn. Magn. Mater. **128**, 93 (1993).
7. O.K. Andersen, O. Jepsen, Phys. Rev. Lett. **53**, 2571 (1984); O.K. Andersen, O. Jepsen, M. Sob, in *Electronic Structure and Its Applications*, edited by M. Yussouff, Lecture Notes in Physics (Springer-Berlin, 1987), Vol. 283; O. Jepsen, O.K. Andersen, Solid State Commun. **9**, 1763 (1971).
8. U. von Barth, L. Hedin, J. Phys. C **5**, 1629 (1972).
9. S. Tougaard, P. Sigmunt, Phys. Rev. B **25**, 4452 (1982).
10. J.J. Yeh, I. Lindau, At. Data Nucl. Data Tab. **32**, 1 (1985).
11. A. Ślebarski, A. Jezierski, L. Lütkehoff, M. Neumann, Phys. Rev. B **57**, 6408 (1998).
12. S. Doniach, M. Šunjić, J. Phys. C **3**, 285 (1970).
13. A.K. See, L.E. Klebanoff, Phys. Rev. B **51**, 7901 (1995).
14. Z. Xu, Y. Liu, P.D. Johnson, B. Itchkawitz, K. Randall, J. Feldhaus, A. Bradshaw, Phys. Rev. B **51**, 7912 (1995).
15. P.D. Johnson, Y. Liu, Z. Xu, D.-J. Huang, J. Electr. Spectr. Rel. Phenom. **75**, 245 (1995).
16. W. Jeitschko, Metall. Trans. **1**, 3159 (1970).